CERN-ACC-2014-0262

HiLumi LHC

FP7 High Luminosity Large Hadron Collider Design Study

FCC-ee Overview

Zimmermann, F (CERN et al)

10 October 2014

The HiLumi LHC Design Study is included in the High Luminosity LHC project and is partly funded by the European Commission within the Framework Programme 7 Capacities Specific Programme, Grant Agreement 284404.

The electronic version of this HiLumi LHC Publication is available via the HiLumi LHC web site <http://hilumilhc.web.cern.ch> or on the CERN Document Server at the following URL: <http://cds.cern.ch/search?p=CERN-ACC-2014-0262>

CERN-ACC-2014-0262

EuCARD-2

Enhanced European Coordination for Accelerator Research & Development

Conference/Workshop Paper

FCC-ee Overview

Zimmermann, F (CERN et al)

10 October 2014

The EuCARD-2 Enhanced European Coordination for Accelerator Research & Development project is co-funded by the partners and the European Commission under Capacities 7th Framework Programme, Grant Agreement 312453.

This work is part of EuCARD-2 Work Package **5: Extreme Beams (XBEAM)**.

The electronic version of this EuCARD-2 Publication is available via the EuCARD-2 web site <http://eucard2.web.cern.ch/> or on the CERN Document Server at the following URL: <http://cds.cern.ch/search?p=CERN-ACC-2014-0262>

FCC-ee OVERVIEW

F. Zimmermann, M. Benedikt, H. Burkhardt, F. Cerutti, A. Ferrari, J. Gutleber, B. Haerer, B. Holzer, E. Jensen, R. Kersevan, P. Lebrun, R. Martin, A. Mereghetti, J. Osborne, Y. Papaphilippou, D. Schulte, R. Tomas, J. Wenninger, CERN, Geneva, Switzerland; A. Blondel, M. Koratzinos, U. Geneva, Switzerland; M. Boscolo, INFN Frascati, Italy; L. Lari, ESS, Lund, Sweden; K. Furukawa, K. Ohmi, K. Oide, KEK, Tsukuba, Japan; S. White, ESRF, Grenoble, France; A. Bogomyagkov, I. Koop, E. Levichev, N. Muchnoi, S. Nikitin, D. Shatilov, BINP Novosibirsk, Russia; U. Wienands, SLAC, Stanford, USA; E. Gianfelice, FNAL, Batavia, USA; L. Medina, U. Guanajuato, Mexico

Abstract

The *FCC-ee* is a proposed circular e^+e^- collider installed in a new 100 km tunnel delivering high luminosity to four experiments at centre-of-mass energies ranging from 91 GeV (Z pole) over 160 GeV (*W* threshold) and 240 GeV (*H* production) to 350 GeV (*t* physics). The *FCC-ee* design is pursued as part of the global Future Circular Collider (*FCC*) study, which regards the *FCC-ee* as a potential intermediate step towards a 100-TeV hadron collider, called *FCC-hh*, sharing the same tunnel infrastructure. We here report the *FCC-ee* design status.

INTRODUCTION

Since 1960 about 30 ring colliders have been successfully built and operated. Many more $e^\pm$ storage-ring light sources have been constructed, with ever smaller transverse emittances. In short, storage rings and storage-ring colliders represent a well understood technology, typically exceeding their design performance within a few years. LEP was the highest energy lepton collider built so far. Its maximum c.m. energy reached 209 GeV, and its total synchrotron radiation power rose up to 23 MW. Figure 1 shows the evolution of the LEP-1/-2 peak-luminosity performance compared with the respective design values, and Fig. 2 the vertical-to-horizontal emittance ratio towards the end of LEP-2. Both figures demonstrate better performance at higher beam energy (increasing over the years).

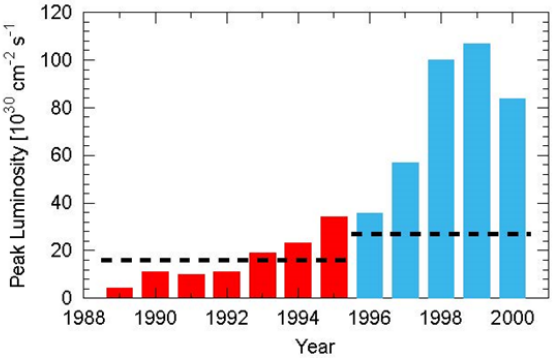

Figure 1: Peak luminosity of LEP-1 (red) and LEP-2 (blue) as a function of year, compared with the respective design values (dashed lines) [1].

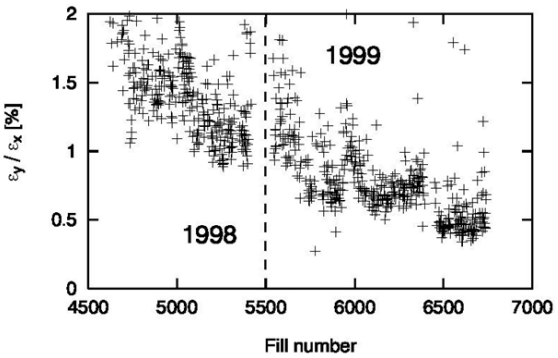

Figure 2: Vertical-to-horizontal emittance ratio at LEP in 1998 and 1999 [1]. The decrease reflects both changes in the damping partition numbers and improved steering [2].

In 1976, B. Richter foresightedly wrote that "An e^+-e^- storage ring in the range of a few hundred GeV in the centre of mass can be built with present technology [and] ...would seem to be ... most useful project on the horizon" [3]. Figure 3, from the same reference, shows the cost-optimized circumference according to 1976 prices as a function of c.m. energy. For 300 GeV c.m. the cost optimum corresponds to a ring of about 90 km in size. This suggests that the 100 km tunnel for a 100-TeV hadron collider also is a good choice for hosting a circular e^+e^- collider operating at up to 350-400 GeV.

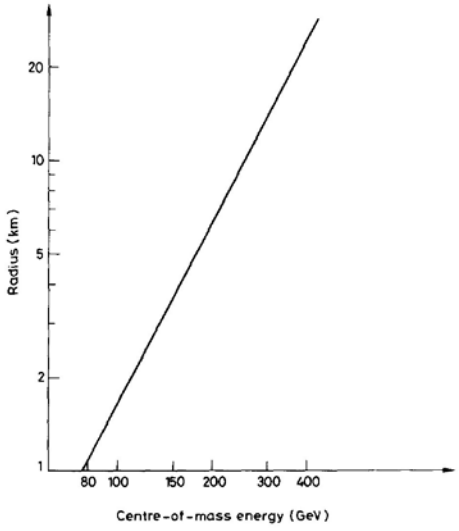

Figure 3: Cost-optimized circumference of a circular e^+e^- collider versus centre-of-mass energy as of 1976 [3].

After first indications and later the confirmed discovery of a Higgs(-like) boson at the LHC, the years 2011 to 2013 have witnessed a revival of Burt Richter's idea, in the form of several new proposals for circular colliders at energies higher than LEP [4-11], such as LEP3 in the LHC tunnel, DLEP at twice the LEP/LHC size, and TLEP in an 80-100 km long tunnel, disucssed in a number of dedicated workshops [12-18].

The 2013 update of the European Strategy for Particle Physics requests CERN to "undertake design studies for accelerator projects in a global context, with emphasis on proton-proton and electron-positron high-energy frontier machines" [19]. This strategy update was formally adopted by the CERN Council.

FCC STUDY

In response to the aforementioned request from the European Strategy, CERN has launched the Future Circular Collider (*FCC*) Study [20], with the mandate to complete a Conceptual Design Report (CDR) and cost review in time for the next European Strategy Update (2018). Presently an international collaboration is being formed with the goal to design a 100-TeV *pp*-collider (*FCC-hh*) together with an 80-100 km tunnel infrastructure in the Geneva area (Fig.4), as well as an e^+e^- collider (*FCC-ee)* as a potential intermediate step, and to also study a *p-e* (*FCC-he*) collider option.

Dipole magnets with a field of about 16 T would allow 100-TeV *pp* collisions in a ring of 100 km circumference. These parameters represent the study baseline.

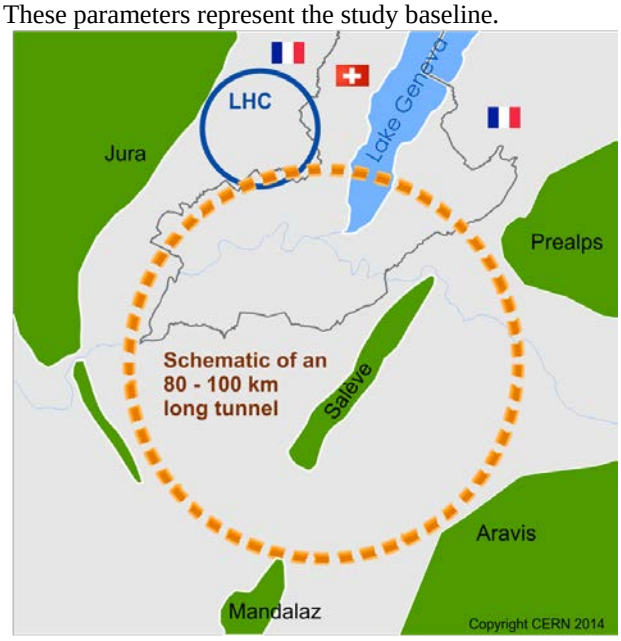

Figure 4: Schematic of an 80-100 km tunnel infrastructure in the Geneva basin.

An FCC kickoff meeting was organized at the University of Geneva on 12-15 February 2014 [21]. More than 340 participants from around the world reflected the widespread interest in the FCC concept and study.The kickoff meeting defined and endorsed the study structure shown in Fig. 5. Collaboration Board and Study Coordination Group have been set up already.

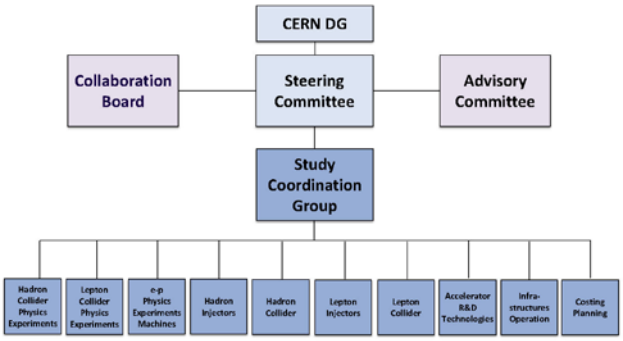

Figure 5: Organization structure of the FCC study.

A preparatory meeting of the collaboration board was held at CERN on 9 and 10 September 2014, with about 80 participants.. L. Rivkin (EPFL & PSI) was unanimously elected as interim Collaboration Board Chair by those institutes which had already formally joined the collaboration. Figure 6 shows the structure of the FCC Study Coordination Group.

Figure 6: The FCC Study Coordination Group.

FCC-hh DESIGN

The physics requirements for *FCC-hh* include highest possible *pp* luminosity at 100 TeV. The present baseline foresees a luminosity of L=5x10^{34} cm^{-2}s^{-1} (as for *HL-LHC*). Higher luminosity appears possible, with implications for pile up, bunch spacing, shielding, cost, etc. In parallel heavy-ion collisions and ion-proton collisions are desired, as for the LHC. Replicating the LHC configuration, four experiments are foreseen, two of which with special purpose detectors. Though proton-beam polarization was successfully demonstrated at RHIC, it is an open question whether polarization can be preserved at the much higher energy of the *FCC*. The baseline beam parameters of *FCC-hh* are summarized in Table 1 [22]. Noteworthy are the figures for the event pile up (number of events per crossing) – which, at the same

luminosity of $5x10^{-34}$ $cm^{-2}s^{-1}$, exceeds the *HL-LHC* value because of a slightly higher cross section –, the total synchrotron radiation power of close to 5 MW (~500 times the LHC value) in a cold environment, and the longitudinal damping time of about 30 minutes (to be compared with half a day at the LHC).

Table 1: Baseline parameters of *FCC-hh* compared with *LHC* and *HL-LHC*.

parameter	*LHC*	*HL-LHC*	*FCC-hh*
c.m. energy [TeV]	14		100
dipole field [T]	8.33		16 (20)
circumference [km]	26.7		100 (83)
luminosity [10^{34} $cm^{-2}s^{-1}$]	1	5	5 [→20?]
bunch spacing [ns]	25		25 {5}
events / bunch crossing	27	135	170 {34}
bunch population [10^{11}]	1.15	2.2	1 {0.2}
norm. transverse emitt. [mm]	3.75	2.5	2.2 {0.44}
Interaction-Point (IP) beta function [m]	0.55	0.15	1.1
IP beam size [mm]	16.7	7.1	6.8 {3}
synchrotron rad. [W/m/aperture]	0.17	0.33	28 (44)
critical energy [keV]	0.044		4.3 (5.5)
total syn.rad. power [MW]	0.007	0.0146	4.8 (5.8)
longitudinal damping time [h]	12.9		0.54 (0.32)

FCC-ee GOALS AND PARAMETERS

The physics requirements for *FCC-ee* comprise highest possible luminosity for a wide physics program ranging from the *Z* pole to the *t* production threshold, at beam energies between 45 and 175 GeV. The main physics programs are: (1) operation at 45.5 GeV beam energy for running at the *Z* pole as "TeraZ" factory and for high precision M_Z and Γ_Z measurements; (2) 80 GeV: *W* pair production threshold; (3) 120 GeV: *ZH* production (maximum rate of *H*'s); (4) 175 GeV: *t-tbar* threshold. Some measurable beam polarization is expected up to ≥80 GeV, which will allow for precise beam energy calibration at the *Z* pole and at the *W* -pair threshold. Key features are the small vertical beta function at the collision point, β_y^*, of only 1 mm, and a constant value of 100 MW for the synchrotron radiation (SR) power assumed at all energies. The power dissipation then defines the maximum beam current at each energy. Eventually a margin of a few percent may be required for losses in the straight sections.

Table 2 compares the baseline parameters of *FCC-ee* with those of LEP-2. For operation at the Z pole an alternative parameter set with almost ten times higher luminosity [24] is also included. The latter considers transversely smaller (lower emittance), but longer bunches (with reduced HOM losses as a welcome side-effect) colliding at 30-mrad crossing angle together with crab-waist sextupoles. Regardless of the collision scheme, the large number of bunches at the *Z*, *W* and *H* energies requires two separate rings, and the short beam lifetime, τ_{beam}, limited by radiative Bhabha scattering at the high luminosity, calls for quasi-continuous injection (top-up).

Table 1: Baseline parameters of *FCC-ee* [23] compared with *LEP-2. For Z* running an alternative scenario based on crab waist collisions is also indicated.

parameter	LEP-2	FCC-ee				
		Z	Z(c.w.)	W	H	t
E_{beam} [GeV]	104	45	45	80	120	175
circum-ference [km]	26.7	100	100	100	100	100
current [mA]	3.0	1450	1431	152	30	6.6
$P_{SR,tot}$ [MW]	22	100	100	100	100	100
# bunches	4	16700	29791	4490	1360	98
N_b [10^{11}]	4.2	1.8	1.0	0.7	0.46	1.4
ε_x [nm]	22	29	0.14	3.3	0.94	2
ε_y [pm]	250	60	1	1	2	2
β^*_x [m]	1.2	0.5	0.5	0.5	0.5	1.0
β^*_y [mm]	50	1	1	1	1	1
σ^*_v [nm]	3500	250	32	84	44	45
$\sigma_{z,SR}$ mm]	11.5	1.64	2.7	1.01	0.81	1.16
$\sigma_{z,tot}$ [mm] (w BS)	11.5	2.56	5.9	1.49	1.17	1.49
hourglass factor F_{hg}	0.99	0.64	0.94	0.79	0.80	0.73
beam-b. p. ξ_y /IP	0.06	0.03	0.175	0.06	0.093	0.092
L/IP [10^{34} $cm^{-2}s^{-1}$]	0.01	28	212	12	6	1.7
τ_{beam} [min]	434	298	39	73	29	21

DESIGN PROGRESS

For the layout of the FCC tunnel various shapes are considered within certain natural boundaries, as indicated in Fig. 7. The geology in the Geneva basin is well suited to housing a circular machine. *FCC-ee* favours a planar design in order to allow for the smallest possible vertical emittance and to minimize depolarizing effects. The required compatibility with hadron collider imposes additional constraints [25], such as on the length of the various straights, the interaction-region (IR) geometry, length and shape of the dispersion suppressors, space needed for hadron collimation etc.

FCC-ee optics modules have been developed for arcs, dispersion suppressors, and various straight sections.

They can be assembled so as to adapt to the overall configuration, e.g. to a circular or racetrack shape of the tunnel. As an example, the arc-cell layout and optics for beam energies of 120 and 175 GeV is shown in Figs. 8 and 9, respectively, with a FODO cell length of 50 m. Figure 10 illustrates an overall circular layout, with 12 straight sections. The dispersion function over 12 km of a circular 100 km ring is presented in Fig. 11, with an arc length of 6.8 km and 1.5 km long straight sections. All of the straight sections accommodate superconducting radio-frequency (RF) systems. At the centre of each arc, a further straight may be inserted.

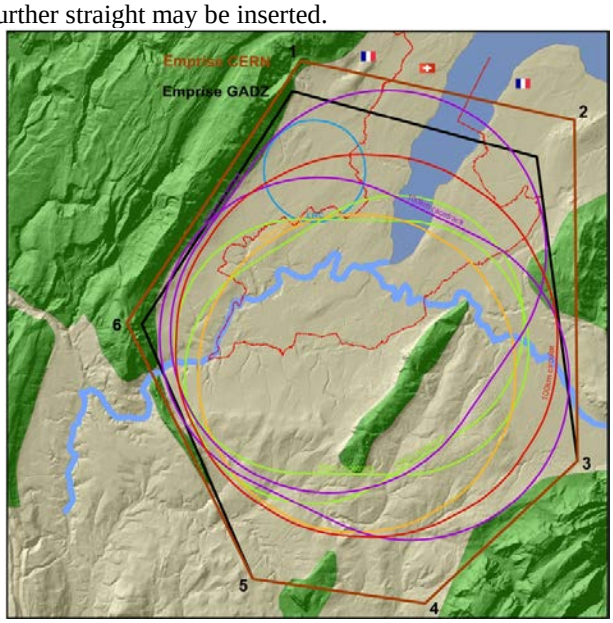

Figure 7: Schematic layouts and boundaries in the Geneva region [26].

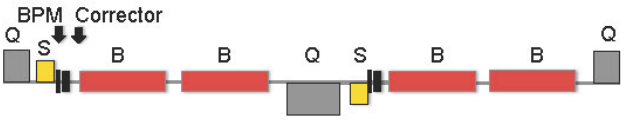

B = bending magnet, Q = quadrupole, S = sextupole

Figure 8: Arc-cell layout for 120 and 175 GeV [27].

At lower energies the arc cell length may need to be increased in order to maintain a reasonably large transverse emittance and acceptable beam-beam tune shifts. The phase advance per cell is another parameter affecting the emittance. Figure 12 displays possible changes in the optics configuration for operation at the *Z* pole. Increasing the cell length by a factor of six appears attractive. Likewise, for operation at the *W*-pair threshold an intermediate cell length of 100 m could be chosen. The corresponding ring optics, over 13 km, for either case are illustrated in Fig. 13. The optics configurations are such that for all energies the horizontal equilibrium emittances due to synchrotron radiation are less than half the design value, leaving margin for the effect of errors and, possibly, high-intensity effects.

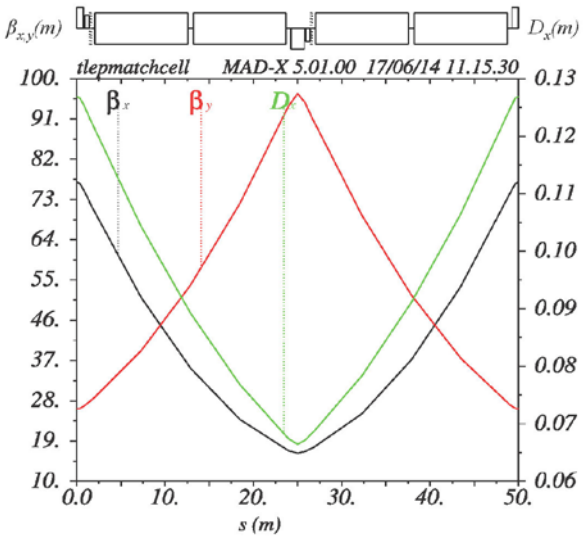

Figure 9: Arc-cell optics at 120 and 175 GeV [27].

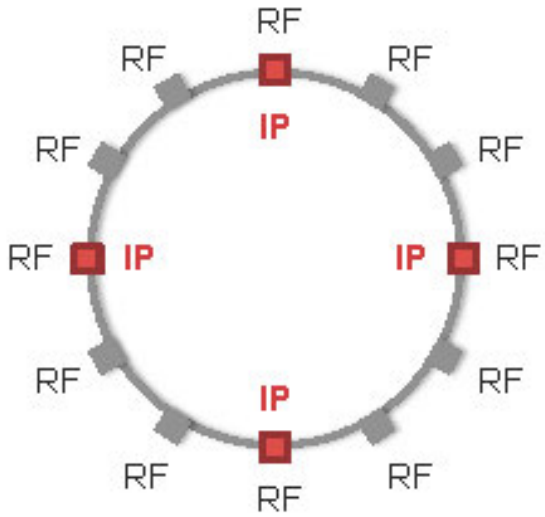

Figure 10: Circular layout with experimental insertions highlighted in red [27].

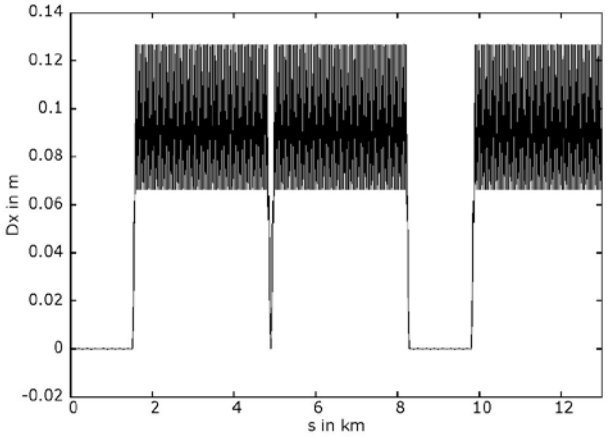

Figure 11: Dispersion function over 12 km including straight sections, for the circular layout of Fig. 10 [28].

Figure 14 shows the SR energy loss per turn as a function of beam energy. For each collision energy this loss translates into a minimum RF voltage, determined by the overvoltage for a decent quantum lifetime and by the momentum acceptance needed with regard to beamstrahlung. At the t-tbar threshold this RF voltage amounts to about 11 GV, which is the maximum voltage considered for the *FCC-ee* design. Operation at 500 GeV c.m. would require a larger RF voltage of 35 GV.

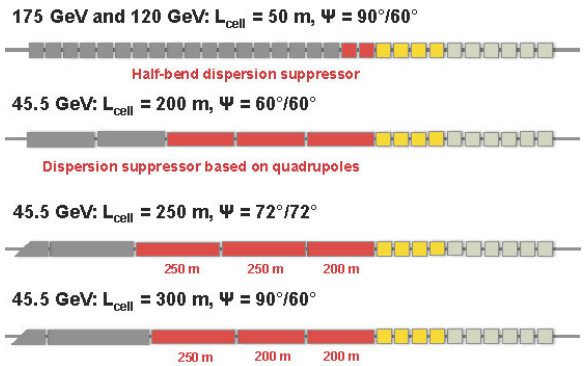

Figure 12: Possible optics configurations at 45.5 GeV compared with the high-energy case (on top). Dark grey color: arc cells; red: dispersion suppressor; yellow: straight matching sections (with RF); light grey: straight sections (with RF) [27].

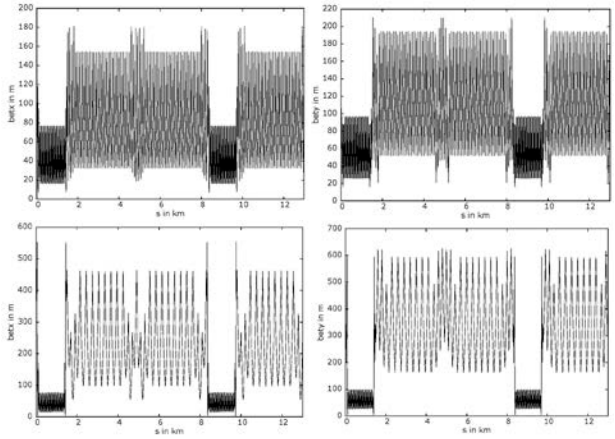

Figure 13: Optics (left: β_x, right: β_y) with 100 (top) and 300-m (bottom) arc cell length for operation at the *W*-pair threshold (80 GeV) and *Z* pole (45.5 GeV energy) [27].

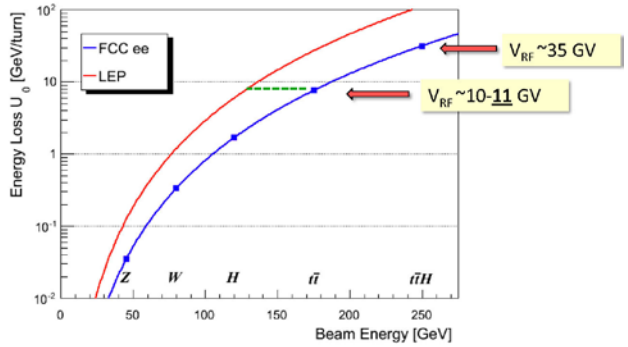

Figure 14: Energy loss per turn as a function of beam energy for *LEP* and for *FCC-ee*, translating into a minimum RF voltage required [29].

The RF system requirements are characterized by two regimes, namely operation at high gradient for *H* and *t* with up to ~11 GV total RF voltage, and high beam loading with currents of ~1.5 A at the *Z* pole. The RF system must be distributed over the ring in order to minimize energy excursions. At 175 GeV beam energy, the total energy loss amounts to about 4.5% per turn and optics errors driven by energy offsets may have a significant effect on the energy acceptance. The *FCC-ee* design aims at SC RF cavities with cw gradients of ~20 MV/m, and an RF frequency of 800 MHz (current baseline). The "nano-beam / crab waist" scheme [24] favors lower frequency, e.g. 400 MHz. The conversion efficiency of wall plug to RF power is critical. R&D is needed to push this efficiency far above 50% (a value achieved at LEP-2).

Concerning the synchrotron radiation it is noteworthy that SR heat per meter at the *FCC-ee* is lower than for many operating rings. For example, the *FCC-ee* SR heat load per meter is more than 10 times lower than for PEP-II or SPEAR (albeit with higher photon energies) [30]. The hard SR spectrum with a critical energy around 1 MeV calls for an efficient absorber and shielding system. A preliminary design is shown in Fig. 15, together with results of pertinent FLUKA simulations in Fig. 16.

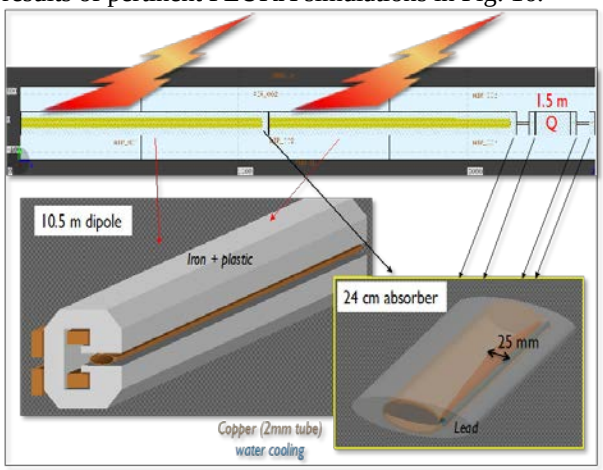

Figure 15: FLUKA geometry layout for half a FODO cell, showing dipole details with a preliminary absorber design including a 5-cm external *Pb* shield [31].

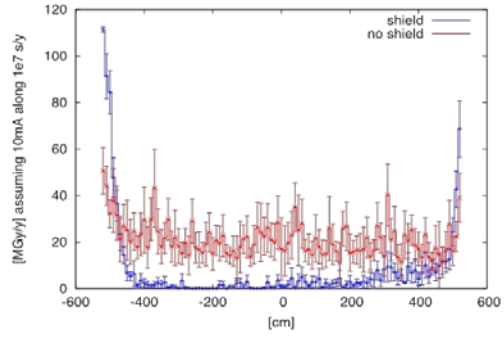

Figure 16: Simulated longitudinal peak-dose profile without (red) and with absorbers (blue) after operating with 10 mA beam current at 175 GeV over a time of 10^7 s (116 days, or one "Snowmass year") [31].

The design luminosities are achieved with $\beta_y^* = 1$ mm, a value so small that it requires a local chromaticity correction. The corresponding IR design is inspired by linear collider final-focus systems. Unlike for the latter, here the beam does not pass the IR only once, and, therefore, the accumulated effect of optical aberrations, including in the non-IP betatron phase, become important. In addition, the local correction implies bending magnets close to the IP, with the associated SR fans. The distance between the IP and the front-face of the first quadrupole, l^*, is currently set to $l^* \geq 2$ m (for SuperKEKB it is ~1 m), with implications for the detector acceptance and luminosity measurement. The combination of the small β_y* and the required large energy acceptance is a challenge. Two preliminary IR designs [32,33] are shown in Figs. 17 and 18, their dynamic apertures in Fig. 19.

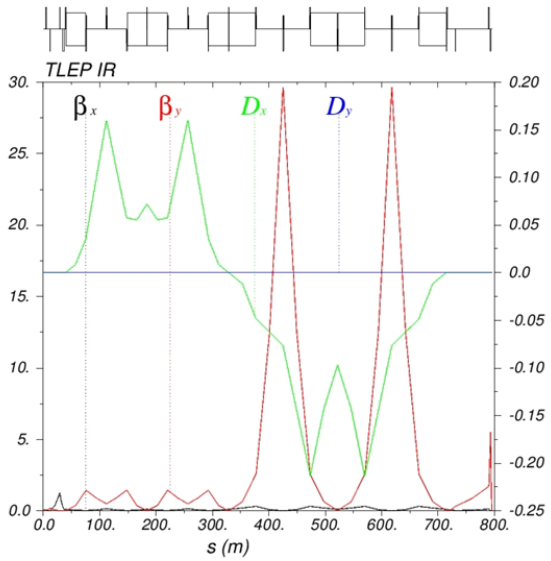

Figure 17: First modular IR design with dedicated chromatic correction sections [32].

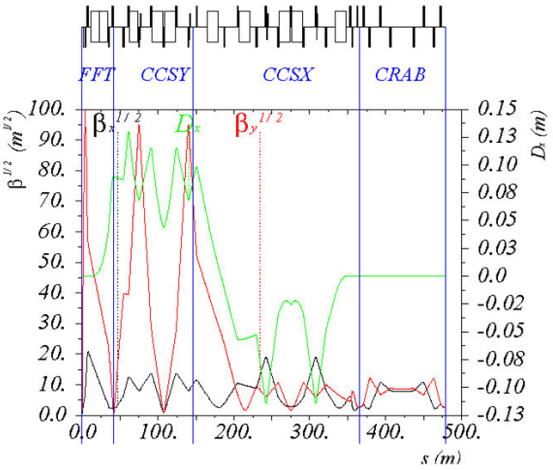

Figure 18: Second modular IR design also including a crab-waist [33].

The challenge for the machine-detector interface is to maximize performance (integrated luminosity) for the experiments with tolerable experimental conditions. This includes minimizing synchrotron radiation in the IR region, by choosing bends as weak as possible and as far as possible away from IP. The final quadrupoles, on the other hand, have to be strong and close to the IP. Their effect is mitigated by minimizing the beam offset from the quadrupole axis, and by controlling vertical halo/tails. The LEP IR, illustrated in Fig. 20, is a good example of an optimized system, with about 100 collimators reducing the machine-induced background, and no direct or singly reflected photons reaching the experiment. A Monte-Carlo model for the synchrotron radiation was integrated into Geant4 [34]. Presently other generic tools are being developed for FCC IR studies [35].

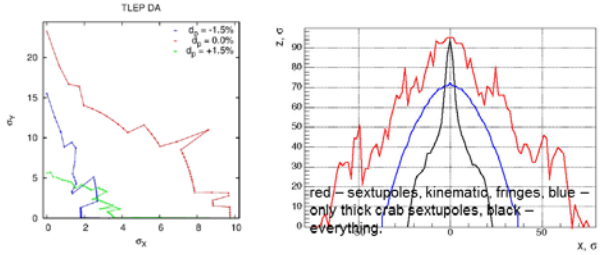

Figure 19: Dynamic aperture at different momentum offsets δ, simulated for the IR optics of Fig. 17 (left) and on-momentum dynamic aperture including setupoles, kinematic terms, fringes, and crab sextupoles for the IR optics of Fig. 18 (right) [32,33].

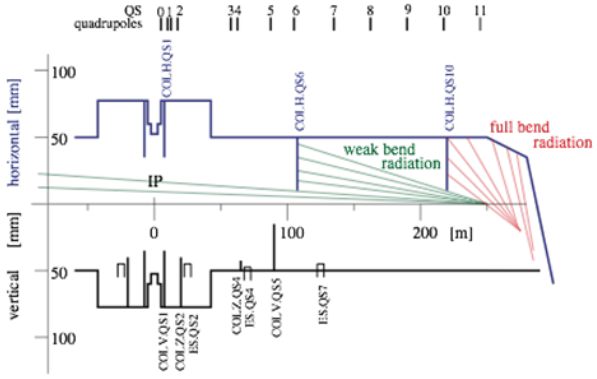

Figure 20: LEP IR design with weak bend and multiple masks [36].

The luminosity of the *FCC-ee* collider can be written as

$$L = \frac{f_{rev} n_b {N_b}^2}{4\pi\sigma_x\sigma_y} HF,$$

where f_{rev} denotes the revolution frequency, n_b the number of bunches per beam, N_b the bunch population, σ_x the horizontal rms IP spot size, σ_y the vertical rms IP spot size, H the luminosity reduction due to the hourglass effect, and F the additional luminosity loss factor due to a crossing angle. The product $en_bN_bf_{rev}$ (with e the elementary charge) is equal to the beam current, which at constant SR power decreases as $1/E^4$. Another constraint comes from the nonlinear beam-beam interaction, the strength of which is characterized by the beam-beam parameter ξ. The vertical beam-beam parameter, roughly equal to the maximum beam-beam tune shift (per IP), is

$$\xi_y = \frac{{\beta_y}^* r_e N_b}{2\pi\gamma\sigma_y(\sigma_x + \sigma_y)} \sim \frac{{\beta_y}^* N_b}{E\sigma_y\sigma_x}$$

The beam-beam parameter is a measure of the tune spread in the beam. According to the experience at all past circular colliders the beam-beam parameter is limited to some maximum value, a fraction of an integer. Using the definition of ξ_y, introducing the limit from the SR power, and neglecting hourglass and crossing-angle effects, the luminosity scaling becomes

$$L \propto \frac{P_{SR}\xi_y}{E^3\beta_y^*}$$

Energy-dependent beam-beam parameter limits for 4 IPs can be scaled empirically from LEP data (Fig. 21), using the inferred relation [37]

$$\xi_{y,max} \propto \frac{1}{\tau^{0.4}} \propto E^{1.2},$$

where τ refers to the radiation damping time. This scaling also is in reasonable agreement with beam-beam simulations for *FCC-ee* [33,38-40].

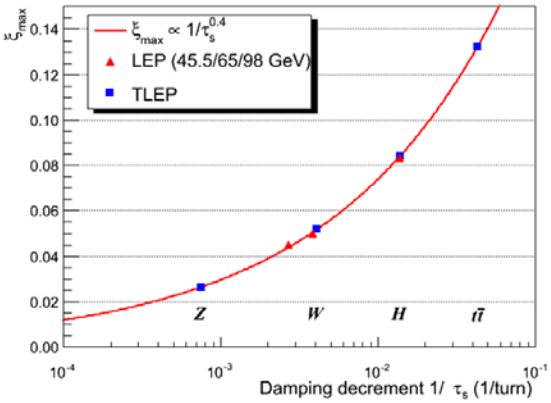

Figure 21: Maximum beam-beam tune shift as a function of damping decrement. Data from *LEP* (red triangles) are extrapolated to the *FCC-ee* (blue squares) according to a physical model [37].

Including the variation of the maximum beam-beam parameter with energy, we finally obtain

$$L \propto \frac{P_{SR}}{E^{1.8}\beta_y^*},$$

i.e. the loss in luminosity with energy is much less dramatic than a naïve look at the SR power might tend to suggest. In addition, the beam-beam limit may be raised significantly with crab-waist collision schemes [24,39,40]. The above scaling is valid as long as the strength of the interaction is dominated by the classical beam-beam interaction. At highest energies a different mechanism may constrain the beam parameters, namely beamstrahlung, i.e. the synchrotron radiation emitted during the collision in the field of the opposing bunch. The hard photon emission at the IPs can become a lifetime or performance limit for large bunch populations (N_b), small horizontal beam size (σ_x) and for short bunches (σ_z). The lifetime due to beamstrahlung depends on the bending radius ρ experienced during the collision,

$$\frac{1}{\rho} \approx \frac{N_b}{\gamma\sigma_x\sigma_z},$$

and on the relative energy acceptance η as [41,24]

$$\tau_{bs} \propto \frac{\rho^{3/2}\sqrt{\eta}}{\sigma_z\gamma^2}\exp(A\eta\rho/\gamma^2),$$

where A is a constant.

To ensure an acceptable lifetime, $\rho\times\eta$ must be sufficiently large, which can be achieved by operating with flat beams (large σ_x), with long bunches, and with a large momentum acceptance of the lattice (about 1.5 – 2% is required; for comparison, LEP had an acceptance of less than 1%, and SuperKEKB is designed for η~1.5%).

The transition from the beam-beam dominated regime to the beamstrahlung-dominated regime depends on the momentum acceptance, as is illustrated in Fig. 22, considering a vertical emittance of 2 pm and β_y^*=1 mm. Figure 23 highlights that the beamstrahlung lifetime is a steep function of the energy acceptance.

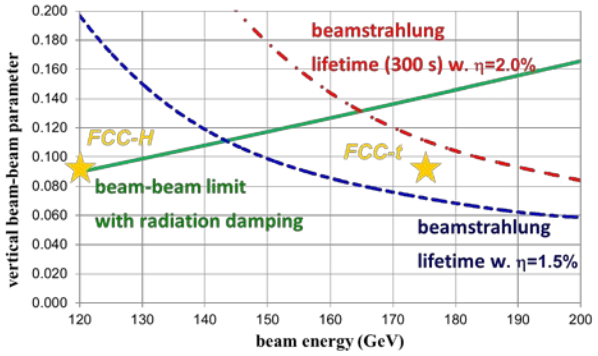

Figure 22: Limits due to classical beam-beam effect and due to beamstrahlung, with two different values for the energy acceptance, as a function of beam energy [42].

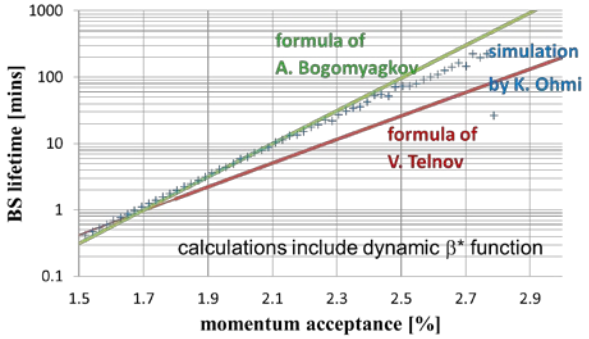

Figure 23: Beamstrahlung lifetime for *FCC-ee* at 350 GeV c.m. as a function of momentum acceptance η, comparing analytical expressions by V. Telnov [41] (red) and A. Bogomyagkov [24] (green) with simulation results from K. Ohmi (blue) [43]. The analytical calculations include the dynamic beta functions matching the simulations.

The β_y^* evolution in e^+e^- colliders since 1980 is illustrated in Fig. 24, which also visualizes how SuperKEKB will pave the way for *FCC-ee*. Figure 25 displays the total *FCC-ee* luminosity (sum over 4 IPs) as a function of c.m. energy. Both the baseline [23] and the improved parameters [24] are shown. The expected high-luminosity values were confirmed in strong-strong and weak-strong beam-beam simulations including the effect of beamstrahlung [39]. For example, in Fig. 26, the

luminosity for *FCC-ee* in Higgs production mode (240 GeV c.m.), simulated by the BBSS code, is $L \approx 7.5 \times 10^{34}$ $cm^{-2}s^{-1}$ per IP, or 25% above the design value. Also, according to BBWS, the luminosity at the Z pole (91 GeV c.m) is indeed much enhanced through the crab-waist scheme, by about a factor of 5, albeit for this case the simulated luminosity of $L \approx 1.5 \times 10^{36}$ $cm^{-2}s^{-1}$/IP still falls slightly short of the expectation [24].

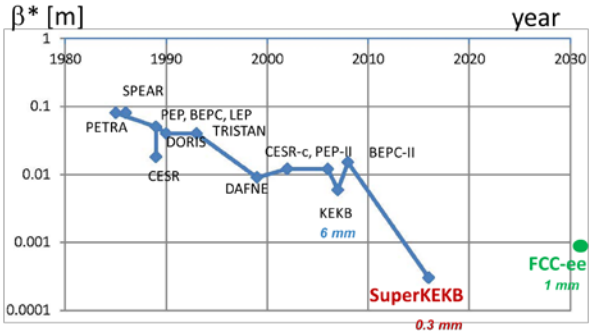

Figure 24: β_y^* evolution over 5 decades.

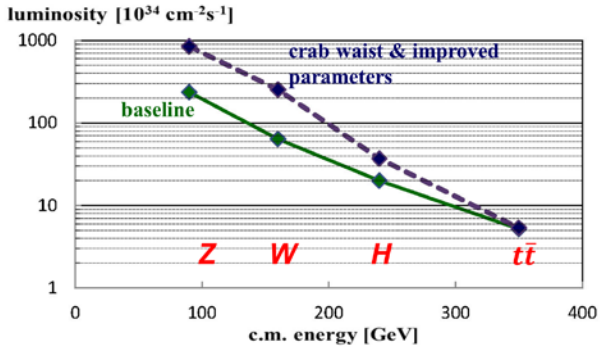

Figure 25: *FCC-ee* total luminosity (4 IPs) vs. c.m. energy – baseline parameters [23] (green solid curve) and crab-waist collision scheme [24] (blue dashed curve).

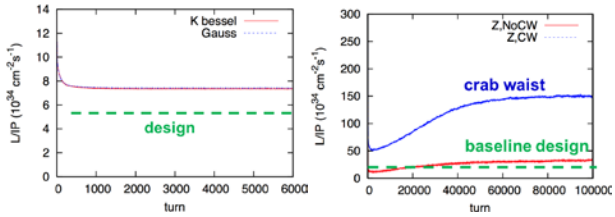

Figure 26: *FCC-ee* beam-beam performance validation including beamstrahlung [39] - BBSS strong-strong simulation at 240 GeV c.m. (left), and BBWS weak-strong simulation at 91 GeV with and without crab waist (bottom). Baseline design values are indicated by the dashed green lines.

SuperKEKB (Fig.27), with beam commissioning to start in 2015, will demonstrate several of the *FCC-ee* key concepts, such as top-up injection at high current; an extremely low β_y^* of 300 μm (*FCC-ee*: 1 mm); an extremely low beam lifetime of 5 min (*FCC-ee*: ≥20 min); a small emittance coupling of $\varepsilon_y/\varepsilon_x$~0.25% (comparable to *FCC-ee*); a significant off momentum acceptance of ±1.5% (similar to the acceptance required for *FCC-ee*); a sufficiently high e^+ production rate of 2.5×10^{12}/s (*FCC-ee* needs less than 1.5×10^{12}/s for top-up operation, at all energies). SuperKEKB goes beyond the *FCC-ee* requirements for many of these parameters.

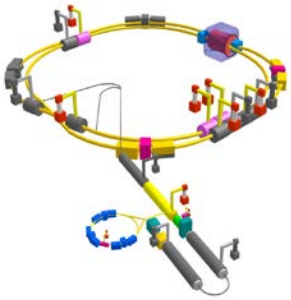

Figure 27: Schematic of SuperKEKB [44].

Beside the collider ring(s), a booster of the same size (same tunnel) must provide beams for top-up injection (Fig. 28). The booster requires an RF system of the same size as the collider, but at low power (~ MW). The top up frequency is expected to be around ~0.1 Hz, and the booster injection energy 10-20 GeV. The booster ring should bypass the particle-physics experiments. Upstream of the booster a pre-injector complex for e^+ and e^- beams of 10-20 GeV is required. The SuperKEKB injector appears to be almost suitable.

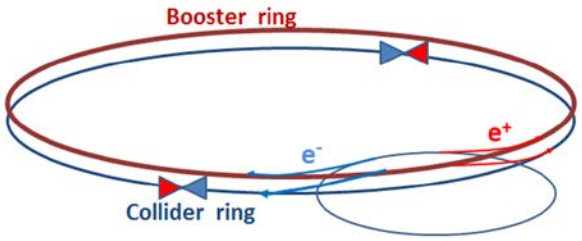

Figure 28: Schematic of booster and collider rings for fast top-up injection [4].

Polarized beams can be of interest for two reasons: (1) they allow for an accurate energy calibration using resonant depolarization, which will be a crucial advantage for measurements of M_Z, Γ_Z, and M_W, with expected precisions of order 0.1 MeV; and (2) they are necessary for any physics programme with longitudinally polarized beams, which would, however, also require that the transverse polarization be rotated into the longitudinal plane at the IP using spin rotators, e.g. as at HERA. Electron integer spin resonances are spaced by 440 MeV.

At LEP the polarization completely disappeared when the energy spread exceeded ~60 MeV (Fig. 29). Noticing that the SR energy spread is proportional to $E^2/\sqrt{\varrho}$ (with ϱ the bending radius), for *FCC-ee* a non-zero polarization is expected up to the *WW* threshold. However, for the same reason (large ρ) at the same beam energy the transverse polarization build-up (due to the Sokolov-Ternov effect) is about 40 times slower than at LEP, e.g. 190 h at the *Z* pole (assuming a ϱ of 11 km); see Fig. 30.

Adding wigglers may lower the polarization time τ_p to ~12 h, limited by the condition $\sigma_E \leq 60$ MeV and the SR power. Dedicated polarization wigglers were proposed and built for LEP [46]. In case of *FCC-ee*, due to the large SR power loss, such wigglers may only be used to pre-polarize some bunches (before the main injection). This will be sufficient for the purpose of energy calibration.

An alternative approach is to generate, accelerate and inject polarized bunches into the collider (requiring snakes in the booster ring, and a self-polarizing positron damping ring) with spins oriented in the horizontal plane [47]. Then the free spin precision frequency could be measured through laser Compton back scattering on the first ~10,000 turns after each injection, with subsequent Fourier analysis, and, thereby, the beam energy be determined. The feasibility of this scheme still needs to be demonstrated.

On the other hand, physics with longitudinally polarized electrons and positrons would require polarization levels of ≥ 40% for both beams, along with excellent resonance compensation. Such physics would also need spin rotators or snakes, and most likely only be possible at (much) lower intensity and luminosity.

Preliminary *FCC-ee* spin tracking simulations are being performed with the code SITROS [48].

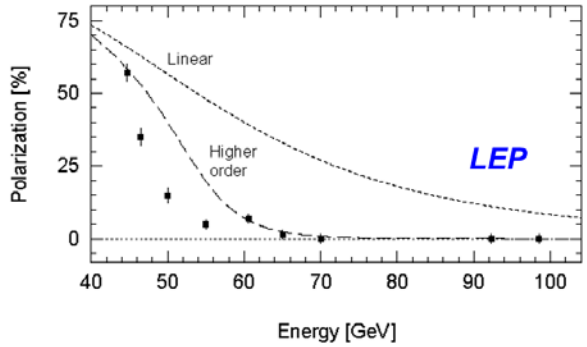

Figure 29: LEP polarization as a function of beam energy. Data points show the measured values. Solid and dashed lines correspond to model predictions [45].

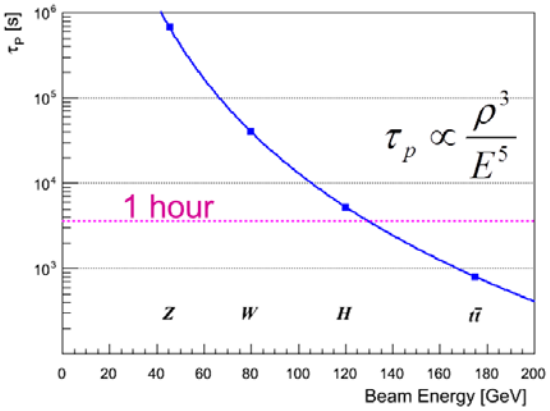

Figure 30: *FCC-ee* natural polarization time versus beam energy [29].

CONCLUSIONS

Colliders and collider designs can look back at a long and successful history, with SuperKEKB set to be the next step. The *FCC* study plan matches the time scale of high-energy frontier physics sketched in Fig. 31. After the kickoff meeting in February 2014, detailed work on the *FCC-ee* design has started. The wide scope of the *FCC* study leaves room for many interesting investigations. At present, the study emphasis is shifting towards parameter optimization and the choice between alternatives. Various technologies need dedicated design efforts, such as magnets, SRF, collimators, vacuum system, etc. The *FCC* study includes colleagues from around the world. The first annual FCC week will be organized in Washington DC, from 23 to 27 March 2015 [49].

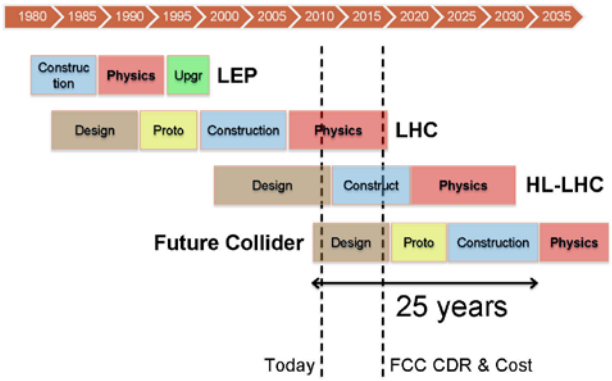

Figure 31: Time line of high-energy physics energy-frontier projects since 1980 with an extrapolation to the Future (Circular?) Collider.

ACKNOWLEDGEMENTS

Our warm thanks go to Weiren Chou for organizing the HF2014 workshop, for inviting a presentation, and for diligently making sure, together with Ning Zhao, that this paper was written and submitted.

This work was partly funded by the European Commission under the FP7 Research Infrastructures project EuCARD-2, grant agreement no.312453.

REFERENCES

[1] R. Assmann, "LEP Luminosity Revisited: Design and Reality," Proc. APAC'01 Beijing (2001)

[2] R. Assmann, P. Raimondi, G. Roy, J. Wenninger, "Emittance Optimization with Dispersion Free Steering at LEP," Phys.Rev.ST – Accel. Beams 3, 121001 (2000).

[3] B. Richter, "Very High Energy Electron-Positron Colliding Beams for the Study of Weak Interactions," NIM 136 (1976) 47

[4] A. Blondel, F. Zimmermann, "A High Luminosity e+e- Collider in the LHC Tunnel to study the Higgs Boson," arXiv:1112.2518v1, 24.12.2011

[5] K. Oide, “SuperTRISTAN - A Possibility of Ring Collider for Higgs Factory,” KEK Seminar, 13 February 2012

[6] A. Blondel et al, “LEP3: A High Luminosity e+e- Collider to study the Higgs Boson,” arXiv: 1208.0504, submitted to ESPG Krakow

[7] P. Azzi et al, “Prospective Studies for LEP3 with the CMS Detector,” arXiv:1208.1662 (2012), submitted to ESPG Krakow

[8] P. Janot, “A Circular e+e- Collider to study H(125),” PH Seminar, CERN, 30 October 2012 ICFA Higgs Factory Workshop: Linear vs Circular, FNAL, 14-16 Nov. ’12

[9] A. Blondel, F. Zimmermann, “Future Possibilities for Precise Studies of the X (125) Higgs candidate,” CERN Colloquium, 22 Nov. 2012

[10] M. Koratzinos et al., TLEP: A High-Performance Circular e+e− Collider to Study the Higgs Boson arXiv:1305.6498 [physics.acc-ph] (2013)

[11] M. Bicer et al., “First Look at the Physics Case of TLEP,” JHEP 1401 (2014) 164

[12] 1st EuCARD LEP3 workshop, CERN, 18 June 2012

[13] 2nd EuCARD LEP3 WS, CERN, 23 October 2012

[14] ICFA Workshop on Accelerators for a Higgs Factory: Linear vs. Circular (“HF2012”), FNAL, 14-16 November 2012

[15] 3rd TLEP3 Day, CERN, 10 January 2013

[16] 4th TLEP workshop, CERN, 4-5 April 2013

[17] 5th TLEP workshop, 25-26 July 2013, Fermilab

[18] 6th TLEP workshop, CERN, 16-18 October 2013, CERN

[19] “The European Strategy for Particle Physics Update 2013,” CERN-Council-S/0106, CERN ESC-E-106 http://cds.cern.ch/record/1567258/files/esc-e-106.pdf

[20] FCC site: http://cern.ch/fcc

[21] Kickoff site: http://indico.cern.ch/e/fcc-kickoff

[22] D. Schulte et al, “Specification: Future Circular Collider Study - Hadron Collider Parameters,” EDMS No. 1342402, FCC-ACC-SPC-0001 v.1.0

[23] J. Wenninger et al., “Specification: Future Circular Collider Study – Lepton Collider Parameters,” EDMS No. 1346081, FCC-ACC-SPC-0003 v.2.0

[24] A. Bogomyagkov, E. Levichev, and D. Shatilov, “Beam-beam effects investigation and parameters optimization for a circular e + e − collider at very high energies,” Phys. Rev. ST Accel. Beams 17, 041004 (2014)

[25] B. Haerer, et al., “Constraints on the FCC-ee Lattice from the Compatibility with the FCC Hadron Collider,” HF2014 Beijing, 9-12 October 2014

[26] J. Osborne, “LHeC Civil Engineering,” LHeC Advisory Committee Meeting, 26 June 2014

[27] B. Haerer, B. Holzer, “Challenges and Status of the FCC-ee Lattice Design,” HF2014 Beijing, 9-12 October 2014

[28] B. Haerer, “ FCC-ee lattices for Different Energies,” FCC-ee Vidyo meeting 25 August 2014.

[29] J. Wenninger, “Lepton Collider Overview,” FCC Kickoff, Geneva 13 February 2014

[30] N. Kurita, “Synchrotron Radiation – Vacuum,” HF2014 [13].

[31] L. Lari, F. Cerutti, A. Ferrari, A. Mereghetti, “Beam-machine Interaction at TLEP: First Evaluation and Mitigation of the Synchrotron Radiation Impact,” IPAC’14 Dresden

[32] H. Garcia et al., “FCC-ee Final Focus with Chromaticity Correction,” IPAC’14 Dresden

[33] A.V. Bogomyagkov, E.B. Levichev, P.A. Piminov “Interaction Region Lattice for FCC-ee (TLEP),” IPAC’14 Dresden; and “Update on IR Design,” FCC-ee Vidyo meeting 23 June 2014.

[34] H. Burkhardt, “Monte Carlo Generation of the Energy Spectrum of Synchrotron Radiation CERN-OPEN-2007-018

[35] M. Boscolo, H. Burkhardt, “Lost particles in the IR and Issues for Beam Induced Backgrounds in Higgs Factories,” HF2014 Beijing, 9-12 October 2014

[36] G. von Holtey et al., “Study of Beam-Induced Particle Backgrounds at the LEP Detectors,” Nucl. Instrum. Methods Phys. Res., A 403 (1998) 205-246

[37] R. Assmann, K. Cornelis, “The Beam-Beam Interaction in the Presence of Strong Radiation Damping,” EPAC’2000 Vienna

[38] S. White, and N. Mounet, “ Beam-Beam Studies for TLEP (and Update on TMCI)," 6th TLEP WS [17].

[39] K. Ohmi, F. Zimmermann, “FCC-ee/CepC Beam-Beam Simulations with Beamstrahlung,” IPAC’14

[40] D. Shatilov, Beam-Beam Effects in High-energy Colliders: Crab Waist vs. Head-On,” HF2014 Beijing, 9-12 October 2014

[41] V. Telnov, “Restriction on the Energy and Luminosity of e+e− Storage Rings due to Beamstrahlung ,” Phys.Rev.Lett. 110 (2013) 114801

[42] M. Koratzinos, “Choice of Circumference, Minimum & Maximum Energy, Number of Collision Points, and Target Luminosity,” HF2014 Beijing, 9-12 October 2014

[43] K. Ohmi, “Beamstrahlung and Energy Acceptance,” HF2014 Beijing, 9-12 October 2014

[44] Y. Ohnishi et al., “Accelerator Design at SuperKEKB,” Prog. Theor. Exp. Phys. 2013, 03A011

[45] R. Assmann, “The Regimes of Polarization in a High Energy e^+e^- Storage Ring,” PAC’99 New York.

[46] A. Blondel and J.M. Jowett, “Dedicated Wigglers for Polarization,” LEP Note 606 (1988)

[47] I. Koop, “Polarization Issues and Schemes for Energy Calibration,” HF2014 Beijing, 9-12 October 2014

[48] E. Gianfelice, “$e^{\pm}$ Collider – Polarization Considerations,” HF2014 Beijing, 9-12 October 2014

[49] FCC Week 2015, site http://cern.ch/fccw2015